9820–9832 *Nucleic Acids Research, 2011, Vol. 39, No. 22* *Published online 14 September 2011*
doi:10.1093/nar/gkr666

Cooperative kinking at distant sites in mechanically stressed DNA

Troy A. Lionberger[1,2,*], Davide Demurtas[3,4], Guillaume Witz[3,5], Julien Dorier[3], Todd Lillian[2,6], Edgar Meyhöfer[1,2] and Andrzej Stasiak[3,*]

[1]Cellular and Molecular Biology Program, [2]Department of Mechanical Engineering, University of Michigan, Ann Arbor, MI, 48109, USA, [3]Centre Intégratif de Génomique, Faculté de Biologie et de Médecine, Université de Lausanne, [4]Centre Interdisciplinaire de Microscopie Électronique, École Polytechnique Fédérale de Lausanne, [5]Laboratoire de Physique de la Matière Vivante, Faculté des Sciences de Base, École Polytechnique Fédérale de Lausanne, 1015 Lausanne, Switzerland and [6]Department of Mechanical Engineering, Texas Tech University, Box 41021, Lubbock TX 79409, USA

Received June 29, 2011; Revised and Accepted July 28, 2011

ABSTRACT

In cells, DNA is routinely subjected to significant levels of bending and twisting. In some cases, such as under physiological levels of supercoiling, DNA can be so highly strained, that it transitions into non-canonical structural conformations that are capable of relieving mechanical stress within the template. DNA minicircles offer a robust model system to study stress-induced DNA structures. Using DNA minicircles on the order of 100 bp in size, we have been able to control the bending and torsional stresses within a looped DNA construct. Through a combination of cryo-EM image reconstructions, Bal31 sensitivity assays and Brownian dynamics simulations, we have been able to analyze the effects of biologically relevant underwinding-induced kinks in DNA on the overall shape of DNA minicircles. Our results indicate that strongly underwound DNA minicircles, which mimic the physical behavior of small regulatory DNA loops, minimize their free energy by undergoing sequential, cooperative kinking at two sites that are located about 180° apart along the periphery of the minicircle. This novel form of structural cooperativity in DNA demonstrates that bending strain can localize hyperflexible kinks within the DNA template, which in turn reduces the energetic cost to tightly loop DNA.

INTRODUCTION

It is now well-established that DNA in both prokaryotic and eukaryotic cells is at least transiently in a negatively supercoiled state (1). DNA supercoiling has been shown to play direct roles in a host of critical cellular processes, including DNA replication, recombination and gene expression (2). An important feature of supercoiled DNA is that the DNA helix is under torsional stress (3). In the case of negatively supercoiled DNA, the helical structure is underwound relative to torsionally relaxed B-form DNA. DNA that is underwound to the extent normally maintained in the cell in some cases undergoes local transitions into alternative DNA structures (4–7). If the DNA template is further untwisted, the torsional energy imparted to the DNA reduces the energetic cost for DNA to transition into alternative, metastable structures, including Z-DNA (8), H-DNA (6) and underwinding-facilitated kinks (9–11). As further detailed below, this article focuses on consequences of strong underwinding on bending flexibility of DNA helix.

DNA regions with reduced local bending stiffness decrease the energetic cost needed to impart high degrees of bending to DNA. Some DNA-binding proteins, for example, are known to form very small DNA loops. One such protein, the lactose repressor (LacI), forms a 93-bp loop that has been shown to contain a region that has transitioned into an alternative, stress-induced DNA structure upon loop formation (12). Should this structural transition enhance the local flexibility of DNA, the energetic

*To whom correspondence should be addressed. Tel: 041 21 692 42 82; Fax: 041 21 692 41 15; Email: Andrzej.Stasiak@unil.ch
Correspondence may also be addressed to Troy Lionberger. Tel: 001 734 764 9421; Fax: 001 734 615 6647; Email: talionberger@gmail.com
Present address:
Troy A. Lionberger, Howard Hughes Medical Institute and Jason L. Choy Laboratory of Single-Molecule Biophysics, Department of Physics, University of California, Berkeley, CA 94720, USA.
Guillaume Witz, Department of Molecular and Cellular Biology, Harvard University, Cambridge MA 02138, USA.

The authors wish it to be known that, in their opinion, the first three authors should be regarded as joint First Authors.

cost for LacI to tightly loop DNA would naturally be reduced as well. In addition to the energetic consequences of stress-induced DNA structural transitions, alternative, non-canonical structures forming in highly untwisted DNA are potent binding sites for many gene regulatory proteins (6,13). However, rigorous experimental efforts seeking to directly implicate stress-induced structures in the activity of certain DNA-binding proteins require that we first develop an understanding of how these alternative structures form and how their appearance alters the mechanical properties of DNA.

Single molecule observations of DNA subjected to significant levels of torque have revealed first insights into structural transitions during which, the DNA double helix exits its elastic regime (14–19). Upon reaching a critical magnitude of torsional stress, a structural phase transition is initiated. This transition leads to the formation of DNA regions with non-canonical, compensatory DNA structures. If strongly untwisted, left-handed L-DNA structures are formed with a helical pitch of about 13 bp/turn (15,20). On the other hand, strong overtwisting of DNA produces right-handed P-DNA structures with a helical pitch of ~2.7 bp/turn (14,15). These compensatory structures act as shock absorbers that 'store' excessive torque while allowing the rest of the molecule to maintain its regular B-DNA structure (21). Once induced, compensatory DNA structures may dynamically respond to changing levels of torsional stress by increasing or decreasing the number of base pairs involved. Importantly, these structural transitions in DNA in response to applied mechanical stresses are in many cases cooperative (18). We expect from previous work that underwinding-induced structural transitions will occur when the twist exceeds -0.6°/bp (15,18) and 1.8°/bp (15) for under and overwound DNA, respectively.

Despite previous efforts to characterize the detailed mechanics of torsionally destabilized DNA, there remains a fundamental gap in our understanding of how the bending mechanics of DNA relates to structural transitions occurring in torsionally stressed DNA. Since DNA in cells is typically both highly bent and twisted, it is crucial that we consider the interplay between these two fundamental, mechanical stresses and structural transitions in DNA. In addition, in order to gain perspective on the possible effects of stress-induced DNA structures might have on the activity of DNA-binding proteins, we must also determine if bending flexibility is conferred to the DNA template, and if so, to what degree. Efforts to address these important questions through direct observation have been limited by two necessary requirements that have not been satisfied in previous studies: (i) DNA must stably sustain known amounts of unwinding and bending during observation and (ii) for the DNA samples investigated, it must be possible to characterize stress-induced structural changes. Here, we seek to provide insight into this unresolved problem by directly observing DNA minicircles using cryo-electron microscopy (cryo-EM). Our cryo-EM observations, in conjunction with targeted nuclease sensitivity assays and Brownian dynamics simulations, have allowed us to identify and characterize the physical properties of torsional destabilizations in DNA.

DNA minicircles provide a convenient and biologically relevant model system that allows us to test the effect of torque-induced DNA transitions on DNA bending. Specifically relevant are DNA minicircles having the size of about 100 bp, since they have a similar radius of curvature as DNA gyres in nucleosomes (22). DNA minicircles of such a small size hardly writhe in response to torsional stress as their high bending stress effectively keeps them in a nearly planar configuration (23–25). In addition, DNA minicircles of this size can exit the elastic torsional regime as a result of an underwinding that is smaller than half of a turn (9). Such an extent of underwinding can be easily achieved during circularization of DNA fragments with the equilibrium twist values that are sufficiently distant from an integer. We used three different DNA minicircles, each sustaining comparable levels of bending but varying levels of torsional stress. Using a DNA nuclease capable of specifically recognizing local disruptions in DNA structure, we verified that the most underwound minicircle is torsionally destabilized. Using cryo-EM, we directly observed that the underwinding-induced structures present in destabilized minicircles confer enhanced bending flexibility, approaching the flexibility of single-stranded DNA (ssDNA). In addition, we performed Brownian dynamics simulations that showed that the levels of flexibility observed are likely to signify a novel mechanism for relieving torsional stress: two kinks appearing at opposing sites along the minicircle periphery. We propose a cooperative model for these structural transitions in which the appearance of one kink triggers formation of a second one through a mechanism that is mediated by bending strain within the template. Our results suggest that DNA bending can preferentially localize the transition of hyperflexible, twist-induced kinks in DNA. The interplay between DNA twisting and bending and the formation of stress-induced kinks, offers a general mechanism for the introduction of localized and well-controlled DNA flexibility that could have implications for many DNA–protein interactions.

MATERIALS AND METHODS

DNA minicircle production

DNA minicircles were prepared as previously described (26). Briefly, the ligation-assisted minicircle accumulation technique (9) was optimized to generate high yields of intact double-stranded DNA (dsDNA) minicircles. Minicircles were formed by the annealing of two ssDNAs (species designated A and B) in which the first half of strand A is complementary to the second half of strand B. Likewise, the second half of strand A is complementary to the first half of strand B. Following annealing, the resulting population of nicked double-stranded minicircles is ligated using a thermophilic (Taq) DNA ligase (New England Biolabs, Beverly, MA, USA). Using a thermocycler, the solution is repeatedly reheated to 95°C for 20 s to melt any DNA that has not successfully formed a closed DNA minicircle, followed by quick reannealing at 4°C for 1 min and ligation at 65°C for 20 min. The solution is then purified of linear DNA

using exonucleases I and III (NEB), and prepared for cryo-EM visualization without further purification.

Bal31 digestion

DNA minicircles were incubated with 0.005 U/ml Bal31 nuclease (NEB) for 10 min at 25°C. The reaction was performed in Bal31 buffer that was used at a 6-fold dilution below manufacturer's recommended buffer conditions (3.33 mM Tris–HCl, 100 mM NaCl, 2 mM $CaCl_2$, 2 mM $MgCl_2$, 0.166 mM EDTA, pH 8.0 at 25°C) to approximate the ionic strength employed previously (9). The reaction was stopped by the addition of 2× urea loading buffer and heat inactivation at 85°C for 10 min. The products were run on pre-cast, denaturing 10% TBE–polyacrylamide gels (7 M urea) (DGel Sciences). The gel was first run at 60 V for 10 min at 55°C (controlled using a recirculating waterbath), and then at 200 V for 480 min. The gel was stained with 1× SYBR Gold stain prior to visualization using ultraviolet *trans*-illumination.

Cryo-electron microscopy

Cryo-EM preparation was performed with the help from a custom-designed plunger as described in detail by Dubochet *et al*. (27). In brief, the DNA minicircles at concentration of ~200 μg/ml (in 10 mM Tris-HCl, 1 mM EDTA, pH 8.0 buffer) were applied to a grid with holey carbon film. After brief blotting with paper filter, the grid was plunged into a cryogen (liquid ethane) that was pre-cooled to the temperature of approximately −160°C. After cryo-vitrification, the specimen was maintained at the temperature of liquid nitrogen during transfer and EM imaging in Philips CM12 electron microscope. The images were taken at the magnification of 45 000 using minimum dose setting and recorded with a Gatan CCD camera. For stereo pairs of images, the specimen holder was tilted by 30° between the two exposures.

3D reconstruction of DNA minicircle shapes

To reconstruct 3D shapes of DNA minicircles from stereo image pairs, we used a program developed previously (28). The program requires that the user aligns two stereo images and then guides the program to localize the reconstructed molecule by identifying several points along the visible axial path of the DNA on both stereo images. With this setting, the program starts its routine of constructing a 3D path that maximally correlates with the signal of the two images, taking into account that the images are projections of the same filamentous object where the tilt angle between the two projections is known (29). The reconstructed axial paths of the minicircles are expressed as lists of points with their x, y and z coordinates in relation to a given reference point. For further analysis, the reconstructed axial paths are resampled (using the spline function of Matlab) to obtain cubic spline lines determined by 150 equally spaced points along each curve.

Brownian dynamics simulations of DNA minicircles with and without hyperflexible sites

The DNA minicircles are simulated adapting Brownian dynamics model, originally proposed by Allison (30) and later improved by other groups (31,32). Minicircles of 34 nm in length (~100 bp) are discretized into $N = 34$ segments of length $l_0 = 1$ nm. The position of vertices and orientation of segments is monitored during the simulation with the help of local reference frames. The displacement of vertices and the rotation of segments obey the standard Brownian dynamics equations. In addition to the random thermal motion, each vertex and segment is subjected to a force field that reproduces DNA mechanics. This force field is derived from three harmonic potentials for: stretching, bending and torsional rigidity as earlier described in detail (31). In addition, a charge is placed on each vertex, and the electrostatic interaction calculated as a Debye–Hückel potential (32).

The conditions used here, correspond to DNA molecules with a persistence length l_p of 50 nm, a torsional rigidity of $C = 300 \times 10^{-21}$ Jnm, and 20 or 50 mM NaCl salt conditions. In real molecules, the persistence length is a product of several interactions such as stacking stabilities and electrostatic interactions, and is largely independent of the ionic conditions (in a reasonably range). For the simulation of long chains composed of long segments (10–20 nm), the electrostatic source of l_p is integrated into the bending rigidity constant, and in turn, no electrostatic interactions are considered between consecutive segments. However, in the case of DNA minicircles with dimensions that are comparable with the Debye radius, this simplification is not allowed. Therefore, the electrostatic interaction is calculated for all pairs of segments with a Debye–Hückel potential, and the bending rigidity constant is reduced to conserve a persistence length of 50 nm. This reduction is of 9.2 or 10.4% for conditions corresponding to solutions with 20 or 50 mM NaCl, respectively, and is calibrated by checking the required reduction of bending rigidity required in the simulation of linear DNA chains to get an effective persistence length of 50 nm.

Molecules with a given ΔLk are simulated by subtracting, at each iteration step, a $2\pi\Delta Lk/N$ angle from each torsion angle between consecutive segments. Molecules with one or two flexible sites are simulated by setting the persistence length of one or two oppositely situated bonds to $l_p = 2$ nm. The iteration step is 5 ps, and 10^8 iterations were performed in each case, i.e. a total time of 500 μs. Ellipticities and bending angles were measured on 10^4 uncorrelated configurations.

RESULTS

Formation of DNA minicircles and estimations of relative torsional stresses

To investigate the effect of varying torsional stress on strongly bent DNA, we decided to study the properties of DNA minicircles with 100, 106 and 108 bp (denoted as MC100, MC106 and MC108, respectively). The complete

sequence of these DNA minicircles was reported previously (26). The sizes of these minicircles differ only by a fraction of one DNA turn, so they will acquire different levels of torsional stress upon formation of covalently closed circles. Conversely, the bending stresses sustained within these minicircles (which is necessarily related to their radius of curvature) is very similar. Based on the earlier work of Du *et al*. (9), we expected 100 bp minicirles to be highly underwound and thus prone to formation of kinks, whereas 106 bp minicircles were expected by us to be nearly relaxed and thus unlikely to form kinks. We expected 108 bp minicircles to show intermediate level of underwinding and we did not know if they should be prone to formation of kinks or not.

Circularization of linear, dsDNA molecules smaller than the persistence length of dsDNA is very inefficient (33). Monomeric DNA minicircles form only rarely, and the ligation products are dominated by dimers and higher oligomers. However, ssDNA has a much smaller persistence length and, consequently, ssDNA that is 100 nt in length can easily circularize (34). Du *et al*. (9) introduced a circularization method based on the annealing of two linear ssDNA molecules that have complementary sequences and are phase-shifted by design so that, the ends of one molecule are brought together by annealing to the central part of the other molecule, and vice versa. The method of Du *et al*. starts with two PCR amplified, linear, blunt-end DNA duplexes that, upon denaturation, produce four ssDNA strands that can anneal to form either the starting blunt-end duplexes (themselves unsuitable as substrates for Taq DNA ligase) or circles with two ligatable nicks placed 180° apart on the circular maps of the formed minicircles. Several denaturation and annealing cycles, each time followed by a 20-min ligation at 65°C by Taq DNA ligase, are needed to convert the majority of the starting material into covalently closed dsDNA minicircles. Using this method, we have prepared DNA minicircles in quantities and purities sufficient for cryo-EM.

In order to determine the magnitude of the torsional stresses sustained within the DNA minicircles we have synthesized, it is necessary to estimate the helical repeat of the linear DNA prior to cyclization because, the extent to which each minicircle is over or underwound is directly related to this value. Numerous studies have established that the helical repeat of DNA can be influenced by DNA sequence, temperature and ionic conditions (35–37) and so, it is important that we consider these variables in our estimation. Under ionic conditions used for standard biochemical experimentation (e.g. 50 mM Tris, 10 mM $MgCl_2$) and at a temperature of 25°C, natural DNA sequences have been reported to have the helical repeat value of 10.54 ± 0.01 bp/turn (24). Recent experiments with DNA minicircles ranging from 105 to 130 bp determined their helical repeat to be 10.54 bp/turn at 21°C (33). Based on these results, it is believed that DNA helical repeat is largely independent of the bending stress in the tested size range of DNA circles (33). Therefore, the helical repeat of the DNA minicircles studied by us is expected to be ~10.54 bp/turn under ambient temperature and in standard buffer conditions. Since our experimental ligation reactions were performed at 65°C, this elevated temperature has to be taken into account while calculating the expected linking number (Lk, or the number of helical turns in DNA) for 100-, 106- and 108-bp long DNA molecules that were cyclized at 65°C (for a brief summary of linking number, see Supplementary Data). At 65°C in a buffer used for standard biochemical experimentation, the DNA of this size is far from its melting temperature. In the temperature interval that does not approach the melting temperature of DNA, the increase of temperature from 21°C to 65°C is expected to decrease the average twist angle between the successive base pairs by 0.0105°/bp/°C (38), which in turn will result in a helical repeat of ~10.68 bp/turn.

Using the temperature-corrected helical repeat of 10.68 bp/turn, we can now estimate the equilibrium linking number (Lk_0) (see Supplementary Data for the definition of Lk_0) and the actual Lk of MC100, MC106 and MC108 during their cyclization at 65°C. For MC100, Lk_0 is expected to be 9.36 and, consequently, these minicircles will attain an Lk of 9 during cyclization because, underwinding by 0.36 turns is less energetically costly than overwinding by 0.64 turns (Figure 1 for schematic presentation of under and overwinding needed to form covalently closed DNA minicircles with 100 bp). For MC106, Lk_0 is expected to be 9.92 and thus, the Lk for the circularized minicircles will be 10 since only a minimal overtwisting would be needed to form this topoisomer. Likewise, the expected Lk_0 for MC108 is 10.11 and the 108-bp minicircles will have an Lk of 10. Analysis of ligation reactions by denaturing gel electrophoresis is

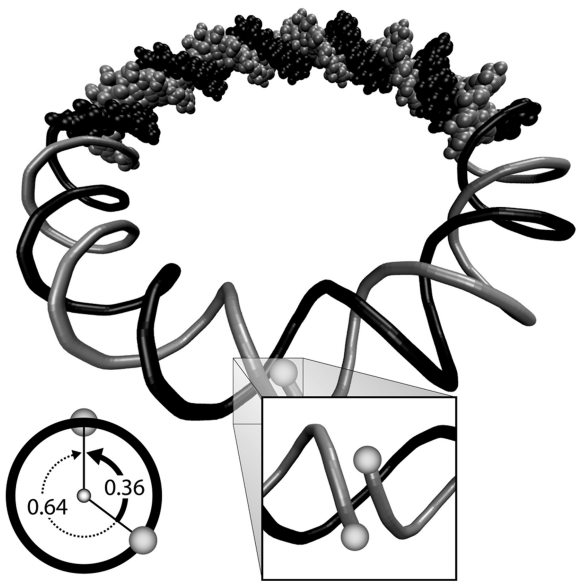

Figure 1. Schematic presentation of a nicked DNA minicircle that has a non-integer equilibrium twist. Covalent closure of the nick can only happen when thermal motion aligns the strand ends (demarked with small spheres). This requires that the DNA molecule either untwists or overtwists by a fraction of a turn. For the case shown, untwisting requires a smaller rotation and is thus energetically less expensive than overtwisting. Therefore, the topoisomer resulting due to DNA untwisting will be much more frequent than that resulting from DNA overtwisting.

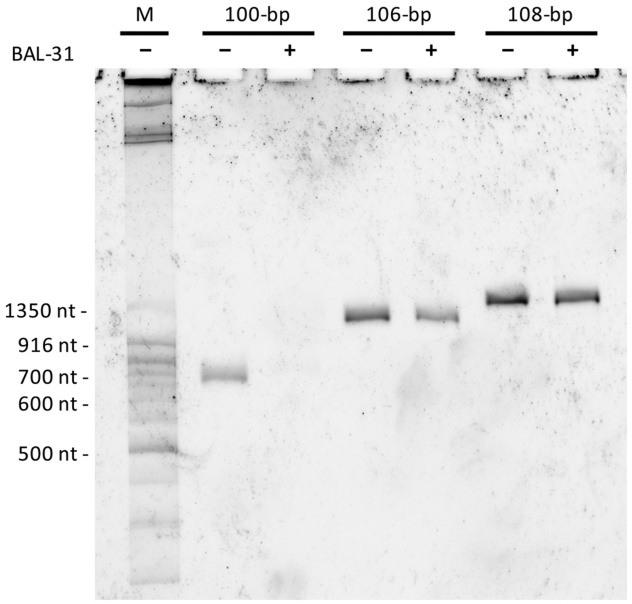

Figure 2. DNA minicircles with 100, 106 and 108 bp, their purity and their susceptibility to Bal31 digestion. In a 10% denaturing PAGE gel (7 M urea), the denatured linear DNA fragments used as a marker, migrate much quicker than circular, covalently closed DNA minicircles in which the two strands cannot separate in space. Notice the presence of only one topoisomer in each category of minicircles and the sensitivity of minicircles with 100 bp to Bal31 nuclease.

consistent with our assumptions and shows that we have obtained only one topoisomer for each of the minicircles (Figure 2).

Detection of kinked DNA by Bal31 sensitivity assays

Bal31 nuclease provides a powerful tool for detecting helix-destabilized DNA. This enzyme does not act on covalently closed dsDNA molecules that are torsionally relaxed (5,39). Bal31 is a known ssDNA exonuclease, capable of endonucleolytic activity on dsDNA containing helical disruptions. Presumably, Bal31 recognizes single-stranded components of melted duplex DNA. Lau and Gray (40) show that torsionally relaxed plasmids are resistant to Bal31 cleavage, whereas, underwound plasmids with superhelical densities as little as −0.02 are recognized as substrates for Bal31. Extremely high levels of overwinding (approximately +0.15) are also capable of producing viable substrates for Bal31 (40). This conclusion trends well with the single molecule observations from Bryant *et al.* (15), which show that overtwisted DNA departs from the elastic regime at torques that are roughly 3.5 times higher than when DNA is untwisted. It is therefore, reasonable to conclude that while the exact structural details of the recognition site for Bal31 are not yet known, the nuclease is capable of at least recognizing helical destabilizations in closed circular substrates. In addition, Lu and Gray note that the degree to which base stacking is interrupted, does not strongly affect the kinetics of Bal31 nuclease activity (41). Therefore, we conclude that recognition by Bal31 likely reflects DNA duplex melting into locally single-stranded complementary strands, but does not provide information about base stacking integrity. Once the covalently closed DNA is cleaved, the exonucleolytic activity of Bal31 completely digests the DNA.

Du *et al.* (9) have used Bal31 nuclease to detect helix-destabilized regions that appeared in highly untwisted DNA minicircles. They have observed that 100-bp minicircles were highly sensitive to Bal31 nuclease, whereas, 106-bp minicircles were virtually resistant. The minicircles studied by us, behaved very similarly to those studied by Du *et al.*, despite having a different sequence. As shown in Figure 2, MC100 proved highly sensitive to Bal31, whereas, MC106 and MC108 (the later size was not investigated by Du *et al.*) were resistant. We interpret these results as indications that the torsional stress sustained in DNA minicircles is sufficient to induce helix destabilization in MC100, but not in MC106 and MC108.

In order to evaluate the degree to which each minicircle was untwisted during the Bal31 assays, we must take into account that these reactions were performed at 25°C. Therefore, the intrinsic twist of DNA should be ∼10.55 bp/turn. For MC100, MC106 and MC108, the corresponding Lk_0 values are expected to be 9.48, 10.04 and 10.23, respectively. Since the linking numbers of the minicircles ligated at 65°C were determined by us to be 9, 10 and 10, respectively (see Supplementary Data), we can conclude that the corresponding ΔLk (i.e. the effective deficit of the number of DNA turns) amount to −0.48, −0.04 and −0.23, respectively, during Bal31 digestion at 25°C. In the case of MC100, the ΔLk of −0.48 indicates that the minicircle is underwound by 173° relative to its equilibrium twist, which corresponds to roughly 1.7°/bp. This value exceeds the critical underwinding angle of 0.6°/bp, which in single molecule experiments resulted in underwinding-induced DNA destabilizations (15). Therefore, it is expected that underwinding within MC100 should result in Bal31 sensitivity. In the case of MC108, a ΔLk of −0.23 means that the DNA is twisted by roughly −0.8°/bp. MC108, therefore, appears at first to exceed the critical unwinding angle needed to destabilize DNA structure. However, it is important to note that the single molecule experiments that determined the critical angle for helix destabilization were performed by keeping linear DNA under a stretching force of 15 pN, so as to avoid the formation of supercoiled plectonemes (15). Applying a stretching force promotes DNA underwinding (18) and so, the critical underwinding angle for DNA molecules subjected to a tensile force of 15 pN is expected to be smaller than that in DNA molecules that are not stretched by external forces.

To estimate how the critical torque varies as a function of applied tension, we turned to the Coulomb–Mohr failure criterion in classical mechanics (42). So long as DNA remains elastic and can be approximated as an isotropic and homogeneous rod, the failure criterion describes the loading conditions (in this case, the tension and torsion applied to free ends of DNA) under which DNA transitions into alternate structural conformations. For clarification, we define failure of DNA not as fracture (as for brittle materials), but rather as the departure from DNA elastic behavior. A calculation of the maximum

shearing stresses (see Supplementary Data) suggests that the critical torque (and hence the critical twist angle) should increase by ~42% in the absence of any tensile loading resulting in a critical unwinding angle of about -0.9°/bp, which would exceed the unwinding expected in MC108. Setting the critical unwinding angle at about -0.9°/bp would explain why MC108 specimens were resistant to Bal31 nuclease under conditions applied here. It is also possible though, that there were helix distortions in MC108 specimens but they were less pronounced and thus, not recognized by Bal31 nuclease. When considering the critical unwinding angle of DNA using classical mechanics theory of elastic rods, one should keep in mind that such treatment at best, approximates what happens to DNA at the atomistic level. In addition, the calculation described above applies for perfectly straight DNA, and any effects of bending are not considered.

Cryo-EM studies of DNA minicircles with kinked regions

To characterize the effect of kinked regions on DNA bending, we directly observed the shape of DNA minicircles by cryo-EM. Cryo-EM has the advantage of permitting visualization of DNA molecules without surface adsorption or staining. Thin layers of DNA solutions are rapidly cryo-vitrified and the molecules maintain the 3D shape they had in solution just before the cryo-vitrification (43). The specimen is then introduced to a pre-cooled, transmission electron microscope and is imaged in the cryo-vitrified state. Two images of the same specimen are taken at two different tilt angles, allowing us to reconstruct the 3D trajectories of individual DNA minicircles from the resulting stereo pair of micrographs (28,43) (Figure 3). For purposes of this study, we assume that the mass of a DNA minicircle is equally redistributed along its contour length, and define ellipticity as the ratio of the lengths of the long and middle principal axes of rotation of the reconstructed 3D shape. As the shapes of reconstructed minicircles were nearly planar (see Supplementary Figure S1), this ratio is very close to the ratio between the lengths of the major and minor axis of a planar ellipse that would best approximate the shape of a given minicircle. The ellipticity is a robust, global parameter that is convenient to calculate from the 3D reconstruction (39).

3D reconstruction of DNA molecules from cryo-EM micrographs is especially delicate for very small DNA molecules. A reconstruction error of the order of just 1 nm can significantly distort the overall shape of DNA minicircles having a radius of ~5 nm. In the case of nearly perfect circles, the reconstruction error can only increase the ellipticity of the reconstructed shapes and thus, acts as a systematic error. The semi-automatic reconstruction program used by us (28) requires user input to indicate several points along the contour of a circular molecule on the two stereo micrographs. The obtained 3D shape is affected by the initial choice of these points. Therefore, independent reconstructions from the same pair of micrographs differ from each other and the root-mean-square deviation (RMSD) between the two reconstructions is of the order of 1 nm (28). In addition, low contrast images, such as these obtained by cryo-EM of unstained DNA molecules create a risk that the reconstruction program may locally trace spurious contaminations producing regions with increased contrast and therefore, result in tracings significantly deviating from the actual contour of DNA molecules. To diminish the possibility that larger than usual reconstruction errors of some molecules could significantly affect the mean parameters of the reconstructed shapes of the investigated DNA minicircles, we decided to eliminate from consideration, the outliers with the ellipticity values exceeding 1 SD from the mean. The outliers constituted up to 30% of reconstructed shapes of a given category of DNA minicircles. The remaining reconstructions are shown in Figure 3 along with their measured ellipticities. We can see that MC106 and MC108 are close to a perfect circle (the ellipticity value of a perfect circle is 1), whereas, the significantly underwound MC100 are highly elliptical. This result indicates that the negative torsional stress sustained within MC100, previously shown to result in sensitivity to Bal31 nuclease, also leads to the creation of easily bendable sites that permit the molecules to minimize their bending energy by adopting elongated, elliptical shapes.

It needs to be added here that by removing outliers from further analysis, we could have also removed the minicircles that indeed showed a shape much different from the typical shape for a given sample as would be the case, e.g. if some of MC100 molecules at the moment of imaging had only one kink. However, as the outliers resulting from reconstruction errors can be interpreted as those resulting from molecules showing less or more kinks, the statistics aimed to quantify the frequency of rare kinking states would be not reliable. For this reason, we focused our analysis on the typical molecules represented in a given sample.

Brownian dynamics simulations of shapes of DNA minicircles with and without hyperflexible sites

Our cryo-EM studies showed that strongly underwound MC100 adopt shapes with the mean ellipticity of about 1.3, while less underwound MC108 and MC106 remain nearly circular and show the mean ellipticity of about 1.1 (Figure 3). As measured by a non-parametric Kolmogorov–Smirnov test, the ellipticity between MC100 and either MC106 or MC108 is significantly different at a confidence limit of 99 and 98%, respectively (Supplementary Table S1). As discussed above, we propose that the high ellipticity of 100-bp DNA minicircles arose as a result of underwinding-induced destabilization of the DNA helix. We hypothesized that these destabilized sites in DNA, in turn, conferred enhanced local bending flexibility to the minicircles. To test this hypothesis, we used Brownian dynamics simulations to systematically explore the effects of introducing highly flexible sites into DNA minicircles.

One important factor determining the shape of small circular DNA molecules is the electrostatic repulsion between DNA segments, which depends directly on the concentration of shielding counterions (salts) in solution. A flexible site will bend less in the presence of a strong repulsive force and therefore, it is important to estimate the

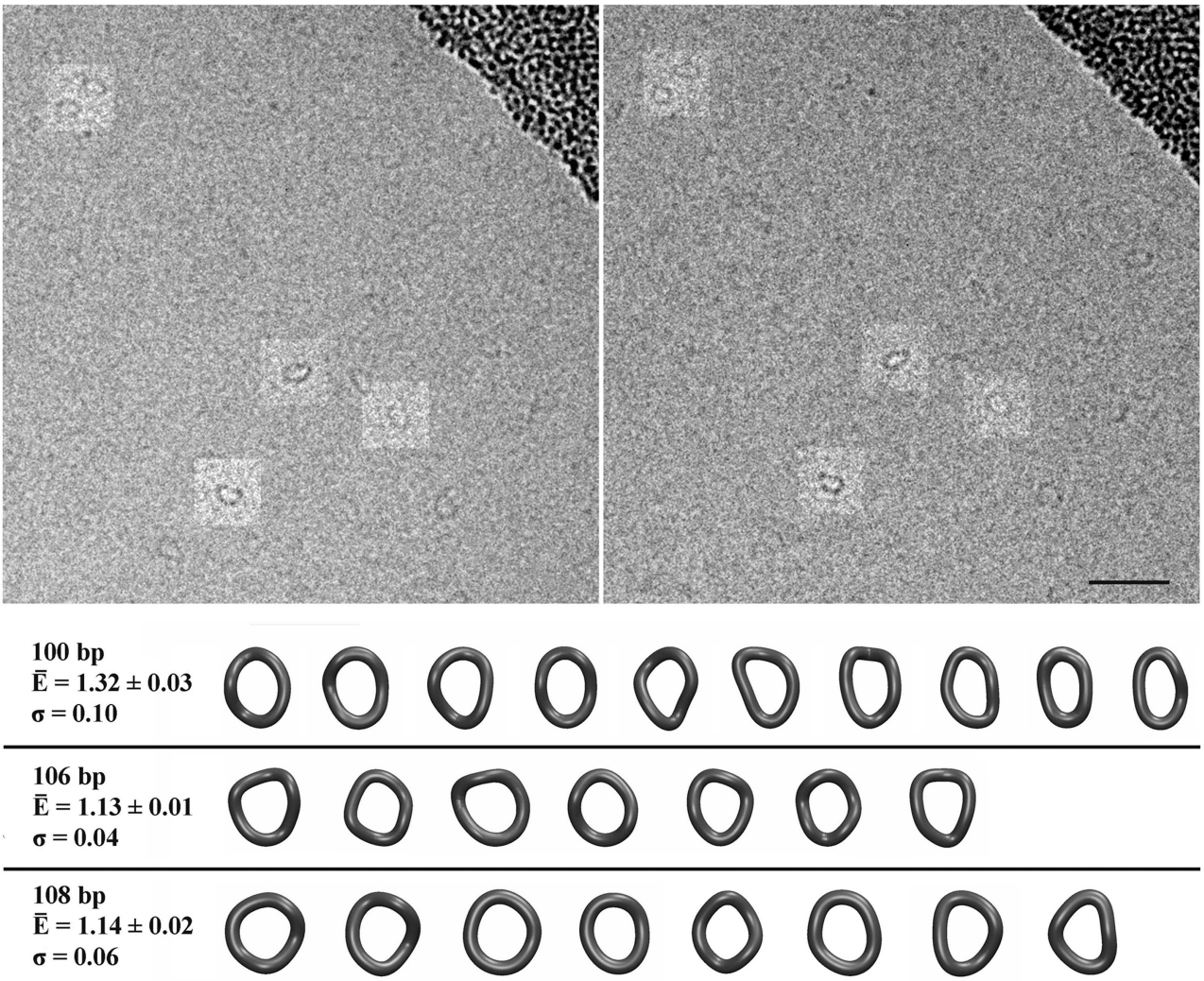

Figure 3. A stereo pair of cryo-EM images of DNA minicircles with 100 bp and a gallery of reconstructed shapes of DNA minicircles with 100, 106 and 108 bp. The mean ellipticity value, the error of the mean determination and the standard deviation (σ) of individual ellipticity values for each type of minicircle is indicted. The magnification bar corresponds to 40 nm. To aid readers to perceive the minicircles on intrinsically low contrast cryo-EM images, some of minicircles are boxed with a region with enhanced contrast.

concentration of counterions in the final state of cryo-EM preparation. For rapid cryo-vitrification during cryo-EM preparation, it is necessary that DNA solutions form very thin films spanning holes in perforated carbon support. Due to the very high surface-to-volume ratio of these thin films, evaporative losses are important and amount to between 50% and 80% of the sample volume during preparation (44). Since salts do not evaporate, their concentration will greatly increase. Unfortunately, it is currently not possible to know the extent of evaporation in individual preparations. Since DNA minicircles were originally suspended in TE buffer (10 mM Tris–HCl, 1 mM EDTA), we estimate that the electrostatic repulsion in imaged specimens corresponds to that experienced by DNA molecules suspended in a solution containing 20–50 mM NaCl. To cover this range of electrostatic repulsion, we performed Brownian dynamics simulations at conditions corresponding to 20 and to 50 mM NaCl.

We first modeled the situation corresponding to that expected for 106-bp minicircles that are torsionally relaxed. Figure 4A shows representative images from such simulations performed under conditions mimicking the effect of 50 mM NaCl. Due to thermal motion, the modeled molecules deviate from perfectly circular configurations and have a mean ellipticity value of 1.126 ± 0.002. Simulations mimicking the effect of 20 mM NaCl gave a slightly lower ellipticity of 1.121 ± 0.002. These ellipticity values agree with those measured for MC106 as measured by cryo-EM and 3D reconstruction.

We, then applied our computational model to the case of MC100, first considering the ellipticity that would be expected if the untwisted DNA minicircle did not contain hyperflexible, stress-induced structures. Figure 4B shows representative images of 100-bp DNA minicircles with ΔLk of -0.5 thermally fluctuating under conditions mimicking the effect of 50 mM NaCl. The modeled molecules very slightly writhed ($Wr \approx -0.016$) but remained largely circular, experiencing a mean ellipticity of 1.140 ± 0.002. Changing the simulation conditions to those corresponding to 20 mM NaCl gave practically the same ellipticity of

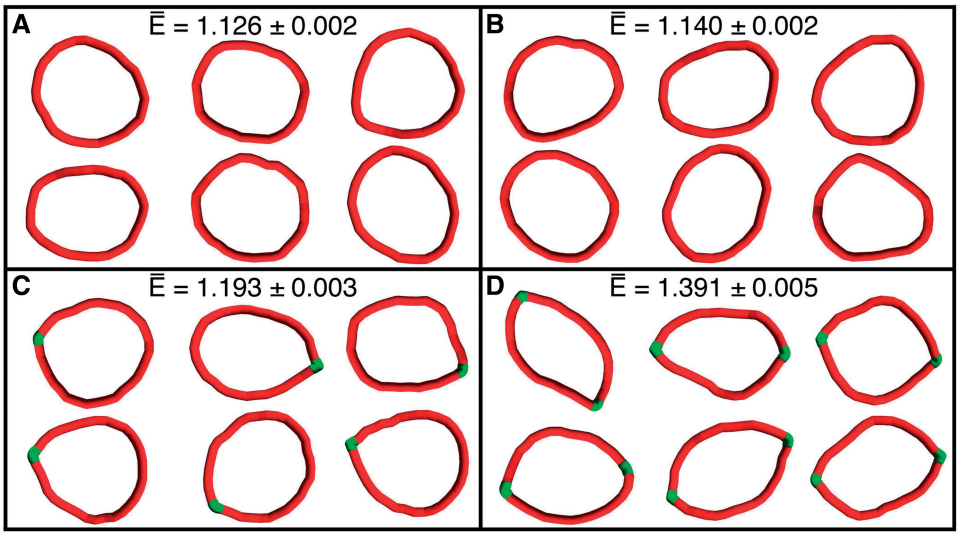

Figure 4. Snapshots from Brownian dynamics simulations of DNA minicircles with and without hyperflexible sites. (**A**) Representative shapes of covalently closed, torsionally relaxed DNA minicircles (situation expected for 106-bp minicircles). (**B**) Shapes of DNA minicircles with $\Delta Lk = -0.5$ that were simulated, assuming that the DNA does not exit its elastic regime. (**C**) Shapes of DNA minicircles with $\Delta Lk = -0.14$ and with one hyperflexible site that is very flexible for bending. (**D**) Shapes of DNA minicircles with two hyperflexible sites placed 180° apart along the circumference of the minicircles.

1.133 ± 0.002. Since the cryo-EM measured ellipticity of MC100 is significantly >1.14, we can discount the formal possibility that MC100 adopt highly elliptical shapes only due to out-of-plane bending (writhing). Importantly, these simulations also establish that the MC100 ellipticity cannot be achieved under thermal energy alone if the DNA structure remains in the elastic regime. These simulation results are not only important for the interpretation of the cryo-EM images of MC100, but also of MC108. As previously discussed for MC108, the ΔLk of -0.23 is likely to be insufficient to induce the formation of kinked sites. The fact that the observed MC108 ellipticity is similar to that of the DNA minicircles modeled as not undergoing kinking, suggests that MC108 (like the torsionally relaxed MC106) does not contain stress induced, distortions of DNA helix that enhance bending flexibility.

To consider the implications of hyperflexible sites appearing in DNA minicircles, we then modeled MC100 that contained one site that is very flexible to bending. The flexible site was modeled as having the flexibility of two ssDNA that are not hydrogen bonded. We observed that, despite the very high flexibility placed at one site in the minicircle, the modeled DNA molecules were much less elliptical than MC100 observed by cryo-EM. We then considered the effects of the torsional stress that could remain in a 100-bp minicircle after two dinucleotide steps transitioned from right- to left-handed helical structure resulting in a change of ΔLk from -0.48 to -0.14. At 50 mM NaCl, the corresponding ellipticity of minicircles modeled with one flexible site and a ΔLk of -0.14 yields a mean ellipticity of 1.193 ± 0.003 (Figure 4 C). At 20 mM NaCl, the ellipticity declines to 1.172 ± 0.003. These results indicate that individual hyperflexible sites in 100-bp minicircles are not sufficient to permit the molecules to take highly elliptical shape with the ellipticity of 1.3 as observed for MC100 (Figure 3).

Interestingly, molecular dynamics (MD) simulations suggested that when DNA minicircles are highly untwisted, two kinks can form at sites located 180° apart, along the circumference of a minicircle (10,45). We therefore modeled a DNA minicircle that contains two highly flexible sites placed diametrically across the minicircle (Figure 4D). The mean ellipticity of these minicircles was measured to be 1.391 ± 0.005 for conditions corresponding to 50 mM NaCl and 1.330 ± 0.004 in the presence of 20 mM NaCl. The later ellipticity value nearly coincides with the ellipticity of MC100 observed by cryo-EM (Figure 3). Our simulations show that the ellipticity values observed by cryo-EM imaging of MC100 can be obtained by accounting for the effects of two highly bendable sites located at opposite sites of the minicircle (Supplementary Figure S2). Therefore, we interpret our results as strongly suggesting that MC100 molecules adopt a structure with two oppositely located kinks.

We were intrigued by the possible formation of two torsionally destabilized regions in MC100, since in general, the junctions between two types of DNA structures, such as B and Z-DNA, e.g. (46), are energetically costly. Therefore, we rather expected one longer region with L-DNA character flanked by two junctions, than two separate, short L-DNA regions with four flanking junctions, in total. Considering possible reasons why minicircles could have two regions, where the DNA exits its elastic regime, we noticed that in our simulated DNA minicircles with one highly flexible site (Figure 4 C), the region that is diametrically opposed to this site experiences a significantly higher bending stress than in minicircles without very flexible bending sites (Figure 5). Therefore, formation of the first kink in a minicircle, despite lowering the overall bending energy of a minicircle, leads to a local increase of the bending stress in the region opposing the kink and may in turn lead to formation of a second kink.

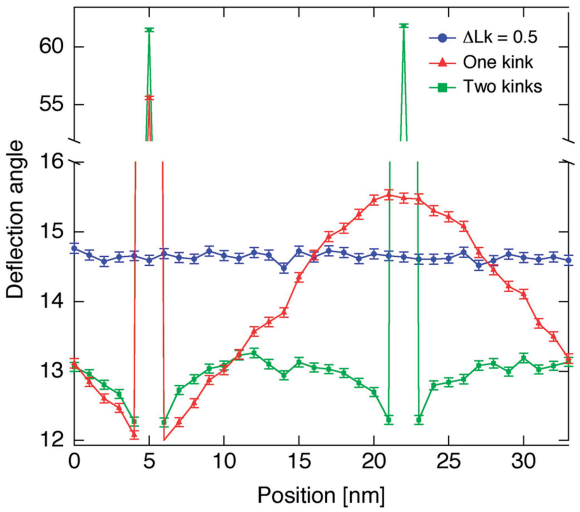

Figure 5. High-bending stress is induced in DNA minicircles in the region placed 180° apart from a highly flexible kink site. Brownian dynamics simulations were used to measure the bending angles between 1 nm-long segments of simulated DNA minicircles. The blue line shows the average bending angles between successive segments measured at sequential 34 vertices of a modeled DNA minicircle with $\Delta Lk = -0.5$ that was simulated, assuming that the DNA does not exit its elastic regime (the situation presented in Figure 4B). The red line shows the corresponding bending angles in modeled DNA minicircles where highly flexible site is placed between segments 4 and 5 (the situation presented in Figure 4C). Notice that a region placed opposite the highly flexible kink shows a higher bending angle than these observed in modeled minicircles that were not permitted to relax their bending stress by formation of a kink. The green line shows the corresponding bending angles in modeled DNA minicircles with two highly flexible sites placed in opposite location (the situation presented in Figure 4D). Notice the bending stress in the remaining portions of the DNA is relieved only after the formation of a second kink.

Considering MC100 a uniformly elastic ring but having one hinge of high flexibility, we calculated that the curvature in the region opposite the hinge should be as high as in torsionally relaxed DNA minicircles with ~76 bp. High curvature of DNA can itself lead to DNA kinking. Du *et al.* (9) determined that the critical DNA curvature that is sufficient to cause DNA kinking, lies between curvature of minicircles with 65 and 85 bp. Therefore, it is possible that the curvature arising in a minicircle after the first kink is sufficient to cause a second kink due to high bending stress alone. Even if the curvature opposite the kink site does not reach the point where the curvature is alone sufficient to cause kinking, one has to take into account that underwound DNA molecules with torsionally destabilized DNA regions still maintain a significant level of unrelaxed torsional stress. Du *et al.* (9) showed that critical bending angle needed to induce kinking is greatly reduced if the molecules are underwound. Therefore, we believe that simulations results presented in Figure 5 support our proposal that, first kinking in DNA minicircles can induce second kinking located 180° apart along the circumference of the minicircle.

We need to stress here that, our simulations only demonstrate the consequences of the presence of flexible regions in the DNA irrespective of their detailed structural characteristics. Based on our simulations, we are unable to say whether the flexible sites have single-stranded character, or are composed of duplex DNA regions with unstacked base pairs. However, based on Bal31 sensitivity of kinked molecules and knowing that this enzyme preferentially acts on DNA regions with single-stranded character, we tend toward an interpretation involving local base separation in at least one of the kinks in doubly kinked minicircles.

DISCUSSION

By circularizing short DNA molecules that differed in their length by a fraction of one helical turn, we obtained DNA minicircles with varying levels of stored torsional energy. DNA minicircles produced with 106 bp (MC106) and 108 bp (MC108) were designed to be less untwisted than their 100-bp counterpart (MC100). In an attempt to assay for the presence of disrupted DNA structures in these minicircles, we incubated each minicircle in the presence of an enzyme (Bal31 nuclease) that is known to specifically digest non-canonical DNA structures. Owing to their resistance to degradation by Bal31 nuclease, we concluded that MC106 and MC108 did not contain torsionally destabilized DNA regions that would be sensitive to Bal31 nuclease. Using cryo-EM imaging in combination with 3D reconstruction, these minicircles were shown to adopt nearly circular shapes. We have further shown through Brownian dynamics simulations that the small levels of ellipticity that were observed in MC106 and MC108 are well within the range that is expected for thermally fluctuating DNA minicircles of this size, even if they are torsionally stressed. In sharp contrast to the less underwound DNA minicircles, MC100 molecules were underwound by nearly half of a helical turn. It is important to note that such a level of underwinding is likely to be higher than that typically maintained in the cell on a global level. However, it has been shown that the degree to which DNA can be locally underwound can be transiently higher than global levels (47). Since locally enhanced levels of torsional stress can induce the formation of non-canonical DNA structures (6,48), MC100 can be used as a model system to study these stress-induced structures under conditions that may be transiently present *in vivo*. As demonstrated here, the elevated level of negative torsional stress in MC100 resulted in the formation of kinked regions that were sensitive to Bal31 nuclease. Based in part on results from previous work characterizing the helical pitch of kinked, untwisted DNA (15), we estimated that disruptions to the helical structure of MC100 should not involve more than two dinucleotide steps due to passing from a right-handed helix with about 10.5 bp/turn to a left-handed arrangement with ~13 bp/turn, the extent of underwinding will be reduced by 62° for each affected dinucleotide stack. As discussed previously, the untwisted MC100 has been estimated to sustain a total twist deficit of 173°. A switch of two dinucleotide stacks from right- to left-handed geometry will reduce the twist deficit to 49°, which would be sufficient to ensure that the twisting angle in the remaining portion of right-handed DNA remains below the critical underwinding angle of

0.6°/bp (15). We observed using cryo-EM that 100-bp DNA minicircles adopted a strongly elliptical shape that is consistent with a model in which kinked sites in DNA are highly flexible to bending. Since MC100 is the smallest of the three minicircles tested, one possible explanation accounting for the appearance of stress-induced, highly flexible sites in MC100 is that the bending energy sustained within the minicircle is sufficient to precipitate the transition into an alternative DNA conformation. However, although MC100 sustains higher magnitudes of bending stress than MC106 and MC108, it was shown by Du *et al*. (9) that 85-bp minicircles do not undergo inelastic kinking due to bending alone. Therefore, it is highly unlikely that the flexible sites observed in MC100 arise simply due to bending alone. We expect that kinking occurs preferentially at sites that are easily meltable; however, the resolution of cryo-EM does not permit us to relate the DNA sequence to observed sites of kinks.

To provide support for our conclusion that kinked regions are highly flexible to bending, we performed Brownian dynamics simulations of DNA minicircles. Our numerical model predicts the 3D shape of DNA minicircles under thermal energy alone, and considers cases where the DNA structure was either uniformly elastic (as with canonical DNA) or contains one or more hyperflexible sites (as we expect for DNA containing localized, kinks). To our surprise, simulations revealed that under the conditions present during cryo-EM, one highly flexible site is not sufficient to permit the modeled DNA minicircles to adopt the degree of ellipticity observed for MC100 (Supplementary Figure S1). Influenced by recent atomistic simulations demonstrating the formation of two kinks in underwound DNA minicircles (10,45), we performed additional Brownian dynamics simulations of DNA minicircles containing two highly flexible sites that are located at opposite points along the circumference of the minicircle. Indeed, the modeled minicircles with two highly flexible sites adopted shapes with similar ellipticities to MC100. Our simulations suggest that the creation of a first hyperflexible site in a DNA minicircle induces high curvature within the region opposite the initial kink, triggering the formation of a second kink in a cooperative manner.

Figure 6 presents our model for structural cooperativity during kinking at distant sites in small DNA loops (also, see Movie S1 in Supplementary Data). Here, we illustrate a 100-bp DNA minicircle that is simulated by a numerical, elastic rod model. As previously discussed, a minicircle of this size is strongly bent but does not kink due to bending alone. As negative torsional stress is increased in this highly bent minicircle, the helical structure of DNA locally destabilizes and a kink is formed (Figure 6A–C). As the bending energy within the entire minicircle equilibrates, the unkinked portion of the DNA adopts a teardrop-like conformation in which the local bending curvature nearest to the kink is reduced and gradually increases as a function of contour distance from the kinked site (Figure 6D). Although the formation of a first kink reduces the overall bending energy within the minicircle, the resulting distribution of bending curvatures localizes the maximal bending stresses in the region of the

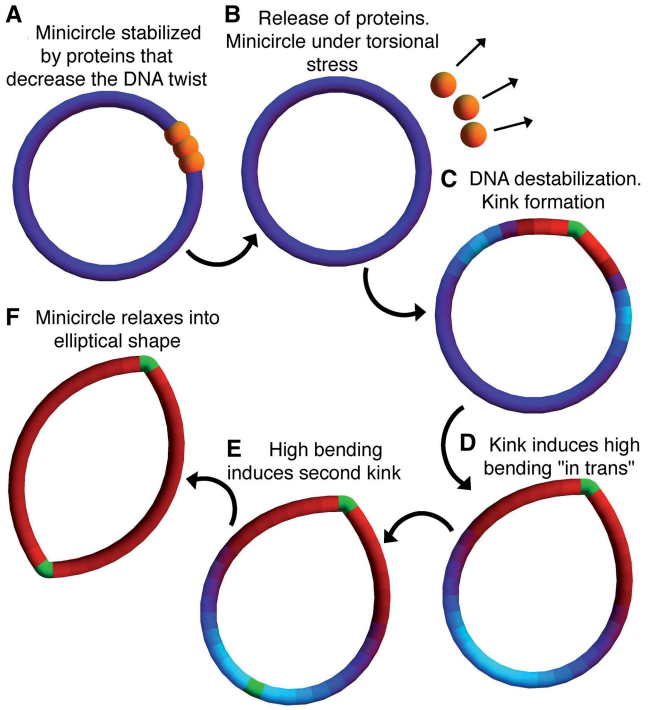

Figure 6. Principle of cooperative kinking. (**A**) In a DNA minicircle with high but subcritical curvature, a flexible site is induced. This site could arise due to kinking resulting, e.g. from dissociation of some proteins that constrain negative supercoiling. (**B** and **C**) Upon formation of a hyperflexible site (kink), the curvature near this site decreases but the curvature in the region placed opposite the kink increases well above the curvature present in the minicircles before formation of the first kink. (**D**) The second kink is formed opposite the first one as soon as this region will reach the critical curvature needed to induce kinking or when the combined effect of bending and torsional stress are sufficient to trigger destabilization of the DNA helix. (**E**) The minicircle relaxes into an elliptical shape, allowing dissipation of the bending strain. The curvature is color coded from red (low) to blue (high) and the flexible junctions are shown in green. The images represent selected images from an animation obtained using our Brownian dynamics simulation where, for the purpose of eliminating contributions from thermal energy, we have set the temperature to 0°K. The entire animation is available as Movie S1 in Supplementary Data.

minicircle farthest from the first kink (Figure 6E). This concentrated, local bending stress, in turn, provides an energetic bias for a second kink to form opposite the first kink (Figure 6F). It should be noted that this process would only be enhanced by negative torsional stress remaining in the minicircle after formation of the first kink.

Our interpretation that underwound 100-bp minicircles adopt configurations with two diametrically opposed kinks originated from numerical simulations using Brownian dynamics. However, these simulations are fundamentally a coarse-grained approach that may not adequately reflect structural changes at the level of individual base pairs. Very recently, Mitchell *et al*. (10) applied atomistic simulations to investigate the effect of torsional stress on DNA minicircles that were ~100 bp in size. DNA minicircles that were underwound comparably with MC100 revealed local torsional destabilization in which, two consecutive base stacks switched from right- to left-handed winding (10). This number of switched stacks

corresponds to our estimation taking into account the torsional relaxation induced by changing from right-handed B-DNA to a left-handed structure with ~13 bp per left-handed turn (15). However, during the simulation time of 50 ns, the DNA minicircles (starting from a perfect circle) were not observed to form kinks. Presumably, the process of kinking requires a longer time than was explored during these simulations. Interestingly, Mitchell *et al.* (10) also simulated DNA minicircles that were more highly underwound, considering minicircles with ΔLk values of -1 and -1.5. These molecules did undergo kinking at two diametrically opposed sites during the simulated time of 50 ns, which is consistent with our model for structural cooperativity. Though the torsional energy in these minicircles was clearly much higher than the minicircles we have observed by cryo-EM, we consider it possible that the additional torsional energy simply allowed the structural cooperativity to occur in timescales capable of being simulated using atomistic simulations. In this case, we view this result as consistent with our model. Measurements of ellipticity of configurations obtained in these atomistic simulations (coordinates provided by J. Mitchell and S. Harris) revealed that molecules with two kinks have the ellipticity of about 1.3, which is remarkably close to that of 100-bp minicircles as determined by cryo-EM and as simulated by us using Brownian dynamics simulations. We therefore, interpret the minicircle structures modeled by Harris *et al.* as strong support for our contention that underwinding destabilized DNA is highly flexible for bending, and that small DNA loops of about 100-bp kink in cooperative manner, where the first kink triggers the second one occurring at opposite site across the small DNA loop.

Whereas, the physical properties of DNA kinking have been the focus of this study, one can only appreciate the significance of our findings by considering the broader biological framework of the problem. We believe that DNA kinking may play an important role in gene regulation. Small DNA loops that are ~100 bp in size are common regulatory elements, formed by loop-forming repressor proteins (49,50). In these systems, kinked DNA could serve either direct or indirect roles in repressing transcription by RNA polymerase. Kinks may serve direct roles in gene regulation by physically interfering with the processive synthesis of RNA by a transcribing RNA polymerase. The DNA minicircles observed in this study (including the kinked, MC100) were previously used to demonstrate that transcription elongation by T7 RNA polymerase was repressed by the mechanics of tightly looped DNA alone (26), though it remains unclear to what degree (if any) kinked DNA played a role in the observations. DNA kinks may also serve an indirect role in regulating transcription. For example, DNA kinks may play a critical role in the binding of loop-forming repressors by making DNA more flexible to bending and thereby reducing the energetic cost of loop formation. In the case of the lactose repressor (LacI), it is known that the DNA duplex is destabilized in a region near the apex of the 93-bp loop that is formed in the absence of other DNA-binding proteins (12).

In this regard, LacI offers an illustrative example of a model system where stress-induced DNA structures are known to appear. In the study by Becker *et al.* (51), LacI was challenged *in vivo* to form small DNA loops ranging from 63 bp to 91 bp in size. The authors investigated looping by LacI both in the presence and absence of the bacterial histone-like protein HU, which is known to preferentially bind to DNA that is both highly bent (52) and kinked (53). Interestingly, loops formed by LacI were stabilized in the presence of HU (51). The authors also note that DNA looping for the most stable loops does not depend on the size of the loop, contrary to expectations for elastically deforming DNA. It therefore, remains possible that HU simply stabilizes kinks naturally appearing at the apexes of the DNA loops already formed by LacI (12). The possibility that LacI first forms a kinked DNA loop, which is then followed by HU binding, is supported by the observed independence of looping on loop size. That is, if kinks confer significant flexibility to the DNA template, it would be expected that loop formation should be less dependent on the size of the DNA loop. Remarkably, Becker *et al.* also demonstrate that the eukaryotic high mobility group protein (HMG) is capable of partially stabilizing the bacterial loops formed by LacI in *Escherichia coli*, despite the fact that HMG is not endogenous to bacteria. Like HU, HMG proteins have been shown to bind preferentially to distorted DNA structures (54), including highly bent DNA (55). The study by Becker *et al.* supports the possibility that DNA kinks are exploited in the LacI system, both to enhance loop formation by conferring enhanced flexibility and to serve as a specific binding site for DNA-binding proteins that recognize stress-induced DNA structures.

In the context of our cryo-EM study of DNA minicircles, we suggest that the kinks that are known to form by LacI are fundamentally similar in nature to the stress-induced kinks we have observed. We, therefore, propose that kinks sustained within the smallest loops formed by LacI significantly increase the flexibility of DNA, approaching the flexibility of ssDNA. Additionally, since our study addresses fundamental, mechanical properties of DNA, the observation of destabilized structures forming in DNA that is highly bent and underwound raises the possibility that DNA kinking serves an important role in many other systems where DNA-binding proteins are known to significantly distort DNA.

SUPPLEMENTARY DATA

Supplementary Data are available at NAR Online.

ACKNOWLEDGEMENTS

We thank Sarah Harris and Jonathan Mitchell for sharing results of atomistic simulations of strongly unwound DNA minicircles. Xiaozhong Zheng and Alexander Vologodskii are thanked for helpful discussions.

FUNDING

The Swiss National Science Foundation (grant 3103A-116275 to A.S.); National Science Foundation (grant CMMI-0969958 to E.M.). The open access publication charge for this paper has been waived by Oxford University Press.

Conflict of interest statement. None declared.

REFERENCES

1. Calladine,C.R., Drew,H., Luisi,B. and Travers,A. (2004) *Understanding DNA: the Molecule & How it Works*, 3rd edn. Elsevier Academic Press, San Diego, CA.
2. Kanaar,R. and Cozzarelli,N.R. (1992) Roles of supercoiled DNA structure in DNA transactions. *Curr. Opin. Struct. Biol.*, **2**, 369–379.
3. Boles,T.C., White,J.H. and Cozzarelli,N.R. (1990) Structure of plectonemically supercoiled DNA. *J. Mol. Biol.*, **213**, 931–951.
4. Bae,S.H., Yun,S.H., Sun,D., Lim,H.M. and Choi,B.S. (2006) Structural and dynamic basis of a supercoiling-responsive DNA element. *Nucleic Acids Res.*, **34**, 254–261.
5. Gray,H.B. Jr, Ostrander,D.A., Hodnett,J.L., Legerski,R.J. and Robberson,D.L. (1975) Extracellular nucleases of Pseudomonas BAL 31. I. Characterization of single strand-specific deoxyriboendonuclease and double-strand deoxyriboexonuclease activities. *Nucleic Acids Res.*, **2**, 1459–1492.
6. Kouzine,F. and Levens,D. (2007) Supercoil-driven DNA structures regulate genetic transactions. *Front. Biosci.*, **12**, 4409–4423.
7. Kowalski,D., Natale,D.A. and Eddy,M.J. (1988) Stable DNA unwinding, not "breathing," accounts for single-strand-specific nuclease hypersensitivity of specific A+T-rich sequences. *Proc. Natl Acad. Sci. USA*, **85**, 9464–9468.
8. Wittig,B., Dorbic,T. and Rich,A. (1991) Transcription is associated with Z-DNA formation in metabolically active permeabilized mammalian cell nuclei. *Proc. Natl Acad. Sci. USA*, **88**, 2259–2263.
9. Du,Q., Kotlyar,A. and Vologodskii,A. (2008) Kinking the double helix by bending deformation. *Nucleic Acids Res.*, **36**, 1120–1128.
10. Mitchell,J.S., Laughton,C.A. and Harris,S.A. (2011) Atomistic simulations reveal bubbles, kinks and wrinkles in supercoiled DNA. *Nucleic Acids Res.*, **39**, 3928–3938.
11. Zheng,X. and Vologodskii,A. (2009) Theoretical analysis of disruptions in DNA minicircles. *Biophys. J.*, **96**, 1341–1349.
12. Borowiec,J.A., Zhang,L., Sasse-Dwight,S. and Gralla,J.D. (1987) DNA supercoiling promotes formation of a bent repression loop in lac DNA. *J. Mol. Biol.*, **196**, 101–111.
13. Butler,A.P. (1986) Supercoil-dependent recognition of specific DNA sites by chromosomal protein HMG 2. *Biochem. Biophys. Res. Commun.*, **138**, 910–916.
14. Allemand,J.F., Bensimon,D., Lavery,R. and Croquette,V. (1998) Stretched and overwound DNA forms a Pauling-like structure with exposed bases. *Proc. Natl Acad. Sci. USA*, **95**, 14152–14157.
15. Bryant,Z., Stone,M.D., Gore,J., Smith,S.B., Cozzarelli,N.R. and Bustamante,C. (2003) Structural transitions and elasticity from torque measurements on DNA. *Nature*, **424**, 338–341.
16. Celedon,A., Nodelman,I.M., Wildt,B., Dewan,R., Searson,P., Wirtz,D., Bowman,G.D. and Sun,S.X. (2009) Magnetic tweezers measurement of single molecule torque. *Nano Letters*, **9**, 1720–1725.
17. Leger,J.F., Romano,G., Sarkar,A., Robert,J., Bourdieu,L., Chatenay,D. and Marko,J.F. (1999) Structural transitions of a twisted and stretched DNA molecule. *Phys. Rev. Lett.*, **83**, 1066–1069.
18. Strick,T., Allemand,J.F., Bensimon,D., Lavery,R. and Croquette,V. (1999) Phase coexistence in a single DNA molecule. *Physica A*, **263**, 392–404.
19. Bustamante,C., Bryant,Z. and Smith,S.B. (2003) Ten years of tension: single-molecule DNA mechanics. *Nature*, **421**, 423–427.
20. Sarkar,A., Leger,J.F., Chatenay,D. and Marko,J.F. (2001) Structural transitions in DNA driven by external force and torque. *Phys. Rev.*, **63**, 051903.
21. Randall,G.L., Zechiedrich,L. and Pettitt,B.M. (2009) In the absence of writhe, DNA relieves torsional stress with localized, sequence-dependent structural failure to preserve B-form. *Nucleic Acids Res.*, **37**, 5568–5577.
22. Luger,K., Mader,A.W., Richmond,R.K., Sargent,D.F. and Richmond,T.J. (1997) Crystal structure of the nucleosome core particle at 2.8 A resolution. *Nature*, **389**, 251–260.
23. Bates,A.D. and Maxwell,A. (2005) *DNA Topology*. Oxford University Press, Oxford.
24. Horowitz,D.S. and Wang,J.C. (1984) Torsional rigidity of DNA and length dependence of the free energy of DNA supercoiling. *J. Mol. Biol.*, **173**, 75–91.
25. Shore,D. and Baldwin,R.L. (1983) Energetics of DNA twisting. II. Topoisomer analysis. *J. Mol. Biol.*, **170**, 983–1007.
26. Lionberger,T.A. and Meyhofer,E. (2010) Bending the rules of transcriptional repression: Tightly looped DNA directly represses T7 RNA polymerase. *Biophys. J.*, **99**, 1139–1148.
27. Dubochet,J., Adrian,M., Dustin,I., Furrer,P. and Stasiak,A. (1992) Cryoelectron microscopy of DNA molecules in solution. *Method. Enzymol.*, **211**, 507–518.
28. Amzallag,A., Vaillant,C., Jacob,M., Unser,M., Bednar,J., Kahn,J.D., Dubochet,J., Stasiak,A. and Maddocks,J.H. (2006) 3D reconstruction and comparison of shapes of DNA minicircles observed by cryo-electron microscopy. *Nucleic Acids Res.*, **34**, e125.
29. Dustin,I., Furrer,P., Stasiak,A., Dubochet,J., Langowski,J. and Egelman,E. (1991) Spatial visualization of DNA in solution. *J. Struct. Biol.*, **107**, 15–21.
30. Allison,S.A. (1986) Brownian dynamics simulation of wormlike chains. Fluorescence depolarization and depolarized light scattering. *Macromolecules*, **19**, 118–124.
31. Klenin,K., Merlitz,H. and Langowski,J. (1998) A Brownian dynamics program for the simulation of linear and circular DNA and other wormlike chain polyelectrolytes. *Biophys. J.*, **74**, 780–788.
32. Vologodskii,A. (2006) Brownian dynamics simulation of knot diffusion along a stretched DNA molecule. *Biophys. J.*, **90**, 1594–1597.
33. Du,Q., Smith,C., Shiffeldrim,N., Vologodskaia,M. and Vologodskii,A. (2005) Cyclization of short DNA fragments and bending fluctuations of the double helix. *Proc. Natl Acad. Sci. USA*, **102**, 5397–5402.
34. Bucka,A. and Stasiak,A. (2002) Construction and electrophoretic migration of single-stranded DNA knots and catenanes. *Nucleic Acids Res.*, **30**, e24.
35. Anderson,P. and Bauer,W. (1978) Supercoiling in closed circular DNA: dependence upon ion type and concentration. *Biochemistry*, **17**, 594–601.
36. Depew,D.E. and Wang,J.C. (1975) Conformational fluctuations of DNA helix. *Proc. Natl Acad. Sci. USA*, **72**, 4275–4279.
37. Peck,L.J. and Wang,J.C. (1981) Sequence dependence of the helical repeat of DNA in solution. *Nature*, **292**, 375–378.
38. Duguet,M. (1993) The helical repeat of DNA at high temperature. *Nucleic Acids Res.*, **21**, 463–468.
39. Demurtas,D., Amzallag,A., Rawdon,E.J., Maddocks,J.H., Dubochet,J. and Stasiak,A. (2009) Bending modes of DNA directly addressed by cryo-electron microscopy of DNA minicircles. *Nucleic Acids Res.*, **37**, 2882–2893.
40. Lau,P.P. and Gray,H.B. Jr (1979) Extracellular nucleases of Alteromonas espejiana BAL 31.IV. The single strand-specific deoxyriboendonuclease activity as a probe for regions of altered secondary structure in negatively and positively supercoiled closed circular DNA. *Nucleic Acids Res.*, **6**, 331–357.
41. Lu,T. and Gray,H.B. Jr (1995) Kinetics and mechanism of BAL 31 nuclease action on small substrates and single-stranded DNA. *Biochim. Biophys. Acta*, **1251**, 125–128.
42. Gere,J.M. and Timoshenko,S. (1997) *Mechanics of Materials*, 4th edn. PWS Publishing Company, Boston.
43. Bednar,J., Furrer,P., Stasiak,A., Dubochet,J., Egelman,E.H. and Bates,A.D. (1994) The twist, writhe and overall shape of supercoiled DNA change during counterion-induced transition

from a loosely to a tightly interwound superhelix. Possible implications for DNA structure in vivo. *J. Mol. Biol.*, **235**, 825–847.
44. Cyrklaff,M., Adrian,M. and Dubochet,J. (1990) Evaporation during preparation of unsupported thin vitrified aqueous layers for cryo-electron microscopy. *J. Electron Microsc. Tech.*, **16**, 351–355.
45. Lankas,F., Lavery,R. and Maddocks,J.H. (2006) Kinking occurs during molecular dynamics simulations of small DNA minicircles. *Structure*, **14**, 1527–1534.
46. Ha,S.C., Lowenhaupt,K., Rich,A., Kim,Y.G. and Kim,K.K. (2005) Crystal structure of a junction between B-DNA and Z-DNA reveals two extruded bases. *Nature*, **437**, 1183–1186.
47. Mojica,F.J. and Higgins,C.F. (1996) Localized domains of DNA supercoiling: topological coupling between promoters. *Mol. Microbiol.*, **22**, 919–928.
48. Rahmouni,A.R. and Wells,R.D. (1989) Stabilization of Z DNA in vivo by localized supercoiling. *Science*, **246**, 358–363.
49. Choy,H.E. and Adhya,S. (1992) Control of gal transcription through DNA looping: inhibition of the initial transcribing complex. *Proc. Natl Acad. Sci. USA*, **89**, 11264–11268.
50. Muller,J., Oehler,S. and Muller-Hill,B. (1996) Repression of lac promoter as a function of distance, phase and quality of an auxiliary lac operator. *J. Mol. Biol.*, **257**, 21–29.
51. Becker,N.A., Kahn,J.D. and Maher,L.J. 3rd (2005) Bacterial repression loops require enhanced DNA flexibility. *J. Mol. Biol.*, **349**, 716–730.
52. Wojtuszewski,K. and Mukerji,I. (2003) HU binding to bent DNA: a fluorescence resonance energy transfer and anisotropy study. *Biochemistry*, **42**, 3096–3104.
53. Pontiggia,A., Negri,A., Beltrame,M. and Bianchi,M.E. (1993) Protein HU binds specifically to kinked DNA. *Mol. Microbiol.*, **7**, 343–350.
54. Travers,A. (2000) Recognition of distorted DNA structures by HMG domains. *Curr. Opin. Struct. Biol.*, **10**, 102–109.
55. Wolfe,S.A., Ferentz,A.E., Grantcharova,V., Churchill,M.E. and Verdine,G.L. (1995) Modifying the helical structure of DNA by design: recruitment of an architecture-specific protein to an enforced DNA bend. *Chem. Biol.*, **2**, 213–221.